

The current-voltage characteristics of n-InGaZnO/p-Si heterojunctions photodiode

GUOLIANG ZHANG, YUN ZENG*, YONGMING YAN, YONGQING LENG

School of Physics and Microelectronics Science, Hunan University, Changsha, 410082, People's Republic of China

Both the light and dark current-voltage (I-V) characteristics of n-InGaZnO/p-Si photodiodes (PD) fabricated by radio frequency magnetron sputtering of n-IGZO films on p-Si substrates at 25 °C, 200 °C and 400 °C have been studied. The dark I-V characteristic indicates the existence of negatively charged interface states at Si-InGaZn oxide interface layer (IL). A theoretical model with IL included is developed and it is found that this model explains the light I-V characteristics observed here well. According to our model, the unique behavior of these PDs is attributed to the impurity concentration of IGZO film and the low electron mobility and deficiency of conduction electrons at IL which causes electron accumulation at interface.

(Received August 24, 2011; accepted September 15, 2011)

Keywords: Photodiode, RF magnetron sputtering, Photoelectric effect, Interface state

1. Introduction

Potential applications of transparent oxides in optoelectronic devices have attracted much attention in recent years. Some researchers have studied the behavior of transparent oxide/Si heterostructure PD such as ZnO/Si photodiode [1]. The effects of both the deposition temperature and oxygen pressure on this type of PD were also studied [2,3], and most of photocurrents in their works are reflected in S-shaped I-V characteristics. In this work, n-IGZO/p-Si heterojunction PD (short as IGZO/Si PD) was fabricated at 25°C, 200°C and 400°C, respectively. The relationship between the deposition temperature and photoelectrical properties was studied. The I-V characteristics under illumination observed here, V_{sat} decreases as I_{sc} increases with increasing deposition temperature, similar to those of ZnO/Si PDs reported before but deviate from those derived from model neglecting interface states. Since it has been demonstrated by Min-Suk Oh and J.Y. Lee that there is an amorphous oxide layer (~2.5 nm thick) formed at the transparent oxide/Si interface during deposition [4,5], a model of IGZO/Si PD with Si oxide IL is developed to account for these results, which is also suitable for other heterojunctions with IL. In our model, the photo-induced electrons to flow through the interface layer will, therefore, be captured by the interface states and may recombine at IL or flow through the IGZO barrier to induce photocurrent. It is indicated that both the electron mobility and the negatively charged states at IL determine the recombination current and photocurrent as well as partial voltage, by which, the light I-V characteristic is determined.

2. Experimental data

Before being sputtered IGZO film on, p-type Si (100) (8~18 Ω cm, doping approx 10^{15} cm^{-3}) substrates were cleaned by organic solvents and then dipped for 10 min into buffered hydrofluoric acid to remove native oxides. Then, the samples were ultrasonically cleaned with acetone, alcohol and de-ionized water for 15 min. After that, an Al film was deposited onto the backside of the Si substrates by electron beam evaporation to form ohmic contacts. Then, an IGZO film (100 nm) was deposited onto the front of Si substrates by rf magnetron sputtering of an IGZO target (In:Ga:Zn:O=1:1:1:4) with the rf power of 100 W. The distance between the target and substrate was adjusted to be 5 cm, the deposition time was limited to 10 min, and the substrate temperature was set to 25 °C, 200 °C and 400 °C. The growth chamber exhibited a base pressure of 2×10^{-4} Pa, Ar with high purity (99.999%) was used as the sputtering gas and the working pressure was controlled at 0.5 Pa. For ohmic contacts to the n-IGZO film, an indium tin oxide (ITO) film was deposited on the IGZO surface by rf magnetron sputtering at 25 °C for 15 min. The schematic structure of cross-section view of fabricated n-IGZO/p-Si heterojunction PD is shown in Fig. 1. Additionally, there were three IGZO films grown on glass substrate at 25 °C, 200 °C and 400 °C individually for hall measurement.

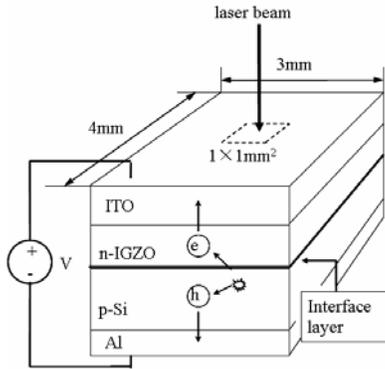


Fig. 1. Schematic structure of cross-section view of n-IGZO/p-Si heterojunction PD.

To avoid the recombination at the perimeter of p-n heterojunction, photoelectrical properties were investigated by the I-V measurements with the illumination of a red laser beam (636 nm wavelength, 450 mW/cm²) into 1 × 1mm² square at the centre of ITO surface. Under 4V reverse bias, the quantum efficiencies as high as 82.1%, 87.97%, and 81.07% are observed for PDs fabricated at 25 °C, 200 °C, and 400 °C, respectively. All the measurements were taken at room temperature (25 °C).

3. Dark I-V characteristics

The I-V characteristics of ITO contacts on IGZO films and those of IGZO/Si PDs in the darkness are shown in Fig. 2a and Fig. 2b respectively. These results show that for all PDs, the formation of ohmic contacts between ITO electrodes and IGZO films and typical rectifying behaviors of PDs are observed. J. P. Donnelly and T. L. Tansley's theory are used to explain the dark current-voltage characteristics of IGZO/Si PDs. Taking into account of interface states, thermally assisted tunneling and emission currents flow through both the wide-gap and narrow-gap material barriers and the total current may be limited by either of them [6]. Considering the division of total junction voltage between the two depletion regions, the voltage dependence of the forward current is given by [7]

$$J \propto \exp(eKV_j/nkT) \quad (1)$$

where V_j is the total applied voltage, K is the fraction of applied voltage dropped across the current limiting depletion region, n is the ideality factor

$$n = \eta \coth(\eta) \quad \text{where}$$

$$\eta = q\hbar/2kT \cdot \sqrt{N/\varepsilon m_e} \quad (2)$$

where N is the impurity concentration, \hbar the Planck-Dirac constant and m_e the effective mass of carrier. To calculate ideality factors, hall effect measurement was performed and the parameters of IGZO film are

summarized in Table 1. At 300 K, the computed value of n equals 1 for Si Schottky diode and 1.15, 2.19 and 3.9 for IGZO Schottky diode as the deposition temperature of IGZO films is 25 °C, 25 °C and 400 °C, respectively. For a p-n junction without interface states, $K \approx 1$ when the Si barrier limits the current or $K \approx 0$ when the IGZO barrier does. It has been proved by T. L. Tansley that, while considering interface states, K may differ from those two ideal values [8]. This is supported by calculation of n/K using Thomas L. Paoli's analog derivative technique which could offset the effect of resistance R_s in series with the n-IGZO/p-Si heterojunction diode [9]. As shown in Fig. 3, the values of R_s were also found out to eliminate the effect of R_s in I-V characteristic under illumination. Since K is in range of 0 and 1, it is clear that, in the case of n-IGZO/p-Si heterojunction PD, the depletion region of Si limits current, interface states are negatively charged, and K is the fraction of applied voltage dropped across the depletion region of Si. It is indicated that interface state influence the dark I-V characteristics of IGZO/Si PD significantly. As reason, we developed a model with considering IL to explain the S-shaped I-V characteristics of IGZO/Si PD, and it is found that interface state also plays important role in determining the light I-V characteristics of IGZO/Si PD.

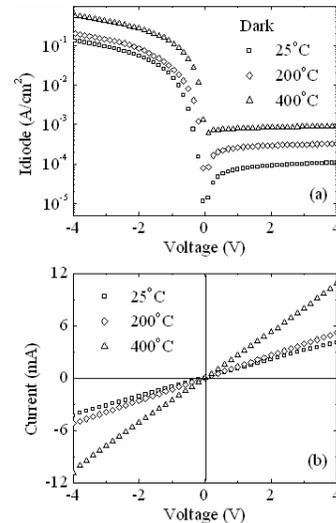


Fig. 2. I-V characteristics of (a) IGZO/Si heterojunction diodes fabricated at 25 °C, 200 °C and 400 °C in the darkness and (b) ITO contacts on IGZO films.

Table 1. Parameters of igzo films deposited at different temperatures.

Substrate Temperature (°C)	Carrier concentration (cm ⁻³)	Mobility (cm ² /Vs)	Resistivity (Ωcm)
25	5.23 × 10 ¹⁸	11.5	5.27 × 10 ⁻¹
200	2.63 × 10 ¹⁹	11.3	6.31 × 10 ⁻²
400	1.12 × 10 ²⁰	10.7	1.18 × 10 ⁻²

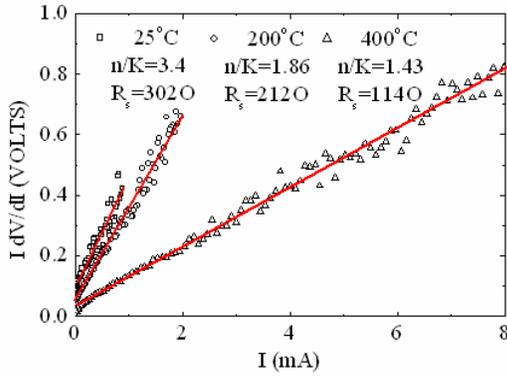


Fig. 3. I_dV/dI against I of IGZO/Si heterojunction diodes fabricated at 25 °C, 200 °C and 400 °C.

4. Light I-V characteristics and discussion

Our model includes the effect of IL and is based on poisson's equation and principle of continuity of electric current. At first, taking into account of interface states, partial voltages, electric field and energy barrier height are calculated. As calculating the photocurrent, both the electron current flowing over and tunneling through the IGZO barrier are included. Since the carrier accumulation at interface is foreseeable, recombination current at both IL and space-charge region (SCR) is considered. Matlab is used to solve the equations, and the results are compared with our experiment results and studied.

4.1 Carrier generation

Since the IGZO film is transparent to the incident light used here, all the photo absorption occurs in silicon. Wolfgang W. Gärtner has pointed out that, the total carriers reach the surface of Si equals to the sum of carriers generated inside the depletion layer (induce drift current J_{DL}) and carriers generated outside the depletion layer in the bulk of Si and diffusing into the reverse-biased junction (induce diffusion current I_{DIFF}) [10]. As shown to the left of Fig. 4, under steady-state conditions, the total photocurrent density at $x=W_i$ is given by [11]

$$I_{TOT} = I_{DL} + I_{DIFF} - I_{RSCR} = qF_l [1 - e^{-aW} / (1 + aL_n)] - qn_0 D_n (n_w / n_0 - 1) / L_n - I_{RSCR} \quad (3)$$

where F_l is the incident photon flux, a the monochromatic absorption coefficient, W the width of the depletion layer, n_w the electron density at $x=W_i$, n_0 the equilibrium electron density, D_n the diffusion coefficient for electrons, L_n the minority carrier diffusion length, and I_{RSCR} the depletion layer recombination current which will be discussed later, respectively. While considering interface states, by which a part of the photo-induced electrons are captured (induce J_c in Fig. 4.a), only the interface electrons with sufficient energy to flow through the IGZO barrier are able to drift into IGZO.

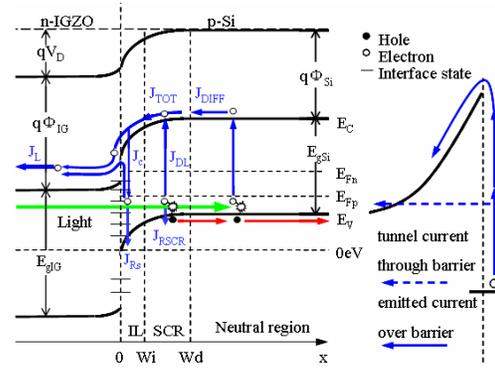


Fig. 4. Energy band diagram of an abrupt n-IGZO/p-Si heterojunction with interface layer and the current-transport mechanisms in n-IGZO/p-Si heterojunction.

4.2. Interface states

If the interfacial capture is efficient, J_c flows in series with and equals to J_{TOT} that all the electrons to flow through the IL will be captured by interface states, the photocurrent is the product of both the amount of interface conductible electrons and the possibility of these electrons flowing into the conduction band of IGZO. The section of Fig. 4 to the right depicts that, the transport process consisting of two contributions; one of them is due to the captured electrons flowing over the IGZO barrier tip, and the other is due to these tunneling through the IGZO barrier.

Here we take the density of interface states to be N_{it} , and assume that the interface states are uniformly distributed across the Si energy gap E_g . The fraction of the interface states that are occupied by electrons is determined by the electron and hole quasi-femi levels E_{fni} and E_{fpi} at interface

$$f_B = \frac{n\sigma_n\nu + p_1\sigma_p\nu}{\sigma_n\nu(n+n_1) + \sigma_p\nu(p+p_1)} \quad (4)$$

where σ_n and σ_p are the capture cross section of electron and hole respectively, n_1 and p_1 the electron and hole density in the conduction band that would exist if the electron and hole Fermi level E_{fni} and E_{fpi} were at interface state Fermi level E_s . Assuming that the thickness of IL W_i is 2nm, N_{it} is constant at IL and the energy of valence band of Si at $x=0$ is 0eV, the total amount of charged interface states is thus found to be equal to

$$N_{filled} = N_{it} W_i / E_g \int_0^{E_g} f_B dE_s \quad (5)$$

According to J. Tersoff's work the Si surface is neutral when the interface states are filled to 0.38 eV, the amount of negative charge at IL N_{charge} is similar to Eq. 5 but with integration from 0.38 eV to 1.12 eV [12].

4.3 Voltage division

By solving the poisson's equation the electric field at IL is obtained as

$$E_i(x) = \sqrt{2qN_{si}V_{si}/\epsilon_{si}\epsilon_0} + N_c \exp\left(\frac{E_{fi} - E_c}{k_0T}\right) \frac{k_0TW_{si}}{V_{si}\epsilon_{si}\epsilon_0} + qN_{charge} \frac{(W_i - x)}{\epsilon_i\epsilon_0} \quad (6)$$

where V_{si} and W_{si} are the partial voltage and the width of depletion layer of Silicon, ϵ_{si} is the dielectric constant of silicon respectively. The first part of Eq. 6 is the electric field induced by majority carrier depletion in SCR using depletion assumption and the second part of that is the additional electric field induced by electron accumulation in SCR with uniform electric field assumption. Therefore, the corresponding maximum electric field in the side of IGZO is determined and the partial voltage of IGZO is found to be

$$V_{igzo} = E_{i(x=0)}^2 \frac{\epsilon_i^2 \epsilon_0}{2qN_{igzo}\epsilon_{igzo}} \quad (7)$$

by which, the energy at the bottom of IGZO conduction band is given by $E_{tbottom} = E_{tip} - qV_{igzo}$ where E_{tip} is the energy at the tip of IGZO conduction band which is 0.87 eV in the case of IGZO/Si heterojunction.

Using the above electric field at IL, partial voltage of IL is thus obtained as

$$V_i = \frac{qN_{charge}W_i^2}{2\epsilon_i\epsilon_0} + E_{i(x=W_i)} \cdot W_i \quad (8)$$

Therefore, the voltage applied on IGZO/Si PD, the sum of V_{igzo} , V_i and V_{si} , is related to E_{fi} which is determined by the current equation which will be discussed later.

4.4 Photocurrent and recombination current

Photocurrent is induced by the interface electrons with sufficient energy to flow over or tunnel through IGZO barrier. The amount of interface electrons with energy to flow over the barrier tip is obtained similar to Ep.5, but with integration from E_{tip} to E_g .

The probability that an electron of effective mass m_{elG} and energy lower than E_t may penetrate the IGZO barrier is given by [7]

$$P_T(y) = \exp\left\{\sqrt{4qm_{elG}\epsilon_{IG}/\hbar^2N_{IG}} \cdot E_t \left[z \ln\left(\frac{1+\sqrt{1-z}}{\sqrt{z}}\right) - \sqrt{1-z} \right] \right\} \quad (9)$$

where E_t is the energy barrier height which equals to qV_{igzo} , y the energy of electron, \hbar the Planck-Dirac constant, z the scaled energy y/E_t , and ϵ_{IG} and N_{IG} are the permittivity and ionized impurity concentration of IGZO, respectively.

Using the fraction of interface states occupied by

electrons and the tunneling probability of interface electron, the transmission coefficient P_t , which represents the fraction of those interface electrons with sufficient energy to flow over or penetrate through the barrier, is given by the sum of possibilities of both processes, i.e.

$$P_t = P_o + P_p = \int_{E_{tip}}^{E_g} f_B dE_s + \int_{\max(E_{tbottom}, 0)}^{E_{tip}} P_T(E_s) f_B dE_s \quad (10)$$

The first and second part of Eq.10 P_o and P_p represent the fraction of electrons flowing over and tunneling through the IGZO barrier, respectively. Thus, the photocurrent induced by interface electrons capable of flowing through the IGZO energy barrier is given by

$$I_L = qP_c P_t E_i(x=0) \mu_i N_{it} W_i / E_g \quad (11)$$

where μ_i is the electron mobility at IL, P_c is a parameter assumed here to define the fraction of conduction IL electrons to total IL captured electrons, in this work we found P_c is suitable in the range of 2.2e-5 to 1.25e-5, through it is arbitrarily chosen to fit the experiment result, it is reasonable considering that neither all of the negative charge is induced by electrons captured nor all of these electrons conduct.

Furthermore, both the recombination currents in SCR and IL are included here

$$I_{RSCR} = \frac{\pi kTW_{si}n_{isi} \exp\left(\frac{E_{fni} - E_{fpi}}{2kT}\right)}{2\tau_n V_{si}} \quad (12)$$

and

$$I_{Ri} = q\sigma_n v_l N_{si} N_{filled} W_i \exp(qV_{si}/kT) \quad (13)$$

where n_{isi} is the intrinsic carrier density of Si, and v_l the mean velocity of electrons at interface, respectively. By equaling the sum of I_L and I_{Ri} to I_{TOT} , the relationship between I_L , E_{fni} and V_{si} is determined. Matlab is applied to solve the equations, and the theoretical results with their corresponding experiment results for PDs made at 25 °C, 200 °C and 400 °C are plotted in Fig. 5 in normalized form by dividing the values of photocurrents by values under 4V reverse bias, respectively.

As shown in Fig. 5, the photocurrent model here including IL fits the experiment results well. Since the principle of I-V characteristic is essential instead of the interface parameters, the IL electron mobility is fixed here to simplify the calculation, curve parameters are P_c and N_{it} . Although these values for parameters u_{si} , 2e-3 cm²/Vsec, S_{int} , 1e-15 cm² and N_{it} are only very rough approximations, they are reasonable values, since the electron mobility in amorphous silicon and capture cross sections in silicon usually range from approximately 10⁻³ to 10⁻¹ cm²/Vsec and 10⁻¹⁶ to 10⁻¹³ cm², respectively.

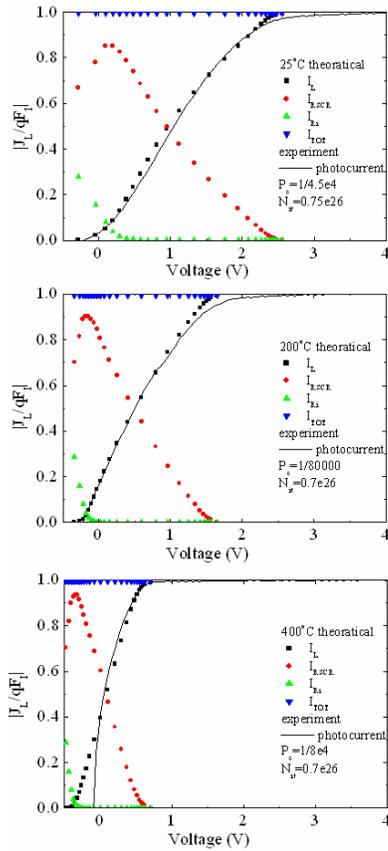


Fig. 5. Normalized experimental and theoretical photocurrent against applied voltage for IGZO/Si heterojunction diodes fabricated at various temperature: (a) 25°C; (b) 200°C; (c) 400°C, the effect of series resistance is eliminated.

It is found that, the interface parameters determine the shape of I-V curve, while interface parameters together with N_{igzo} decide on V_{sat} . The S-shaped I-V characteristic of IGZO/Si PD is caused by high electron recombination at IL and SCR under low reverse bias, with increasing the reverse bias voltage recombination at IL decreases rapidly and the electron recombination occurs mainly at SCR. To highlight the effect of N_{igzo} on V_{sat} , the interface parameters for calculation for 200 °C and 400 °C PDs are kept the same. As shown in Fig. 5, V_{sat} decreases from 1.32V to 0.48V as N_{igzo} increases from $2.63 \times 10^{19} \text{ cm}^{-3}$ to $1.12 \times 10^{20} \text{ cm}^{-3}$. Since V_{igzo} is inversely proportional to N_{igzo} which increases with increasing deposition temperature, it explains why saturate voltage V_{sat} decreases as short-circuit current I_{sc} increases with increasing deposition temperature.

For PDs fabricated at different temperature, the contribution of flowing over and tunneling through currents differs. As shown in Fig. 6a and Fig. 6b, for PDs fabricated at 25 °C and 200 °C, the tunneling through current dominates the photocurrent under low reverse bias. With increasing reverse bias voltage, the flowing over current increases faster than the tunneling through current

and the photocurrent is decided by the flowing over current much more. However, as shown in Fig. 6c, for PDs fabricated at 400 °C, the flowing over current dominates the photocurrent all the time. As reverse bias increases above V_{sat} , the flowing over fraction keeps rising while the tunneling through fraction falls. These phenomena are explained by further observation into the interface electron quasi-femi levels and voltage division. As shown in Eq.9 and Eq.10, the fraction of electrons flowing over barrier is decided by E_{fni} while the fraction of electrons tunneling through barrier is decided by both E_{fni} and V_{igzo} .

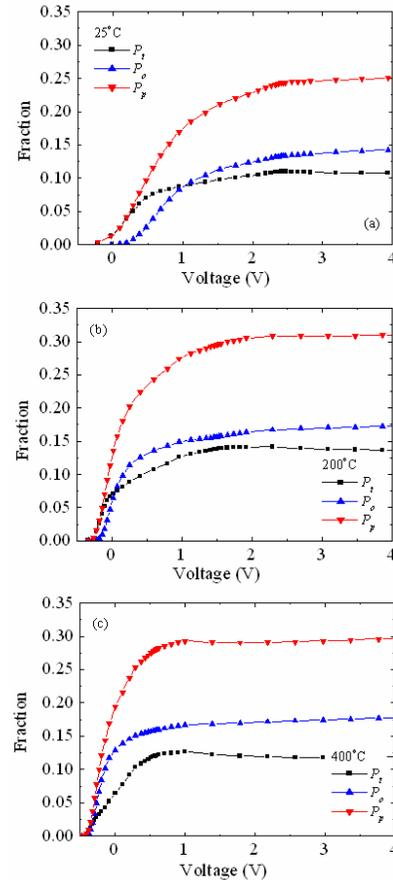


Fig. 6. P_t , P_o and P_p against applied voltage of IGZO/Si heterojunction diodes fabricated at various temperature: (a) 25°C; (b) 200 °C; (c) 400 °C

As shown in Fig. 7, E_{fni} rises as reverse bias voltage increases and saturates near V_{sat} for all PDs. It is easier to understand assuming that the interface below E_{fni} is filled with electron while the state above E_{fni} is empty. As E_{fni} increases, interface state at higher energy is filled with electron, and these electrons above E_{tip} may flow over the IGZO barrier. Since the E_{fni} of PDs saturates under lower reverse bias with increasing deposition temperature, the flowing over fraction increases faster and saturates under lower reverse bias for PDs fabricated at higher temperature. Partial voltage is plotted in Fig. 8, for PD fabricated at higher temperature, more of the reverse bias voltage falls

on the side of Si. As shown in Eq.9, with increasing N_{igzo} , the tunneling possibility increases. However, the reduction of V_{igzo} leads to smaller tunneling through fraction according to Eq.10. Combining the effect of E_{fni} , N_{igzo} and V_{igzo} , the principle of flowing over and tunneling through fraction shown in Fig. 6 is clarified.

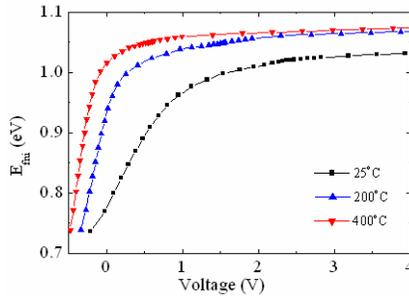


Fig. 7. E_{fni} against applied voltage of IGZO/Si heterojunction diodes fabricated at 25 °C, 200 °C and 400 °C.

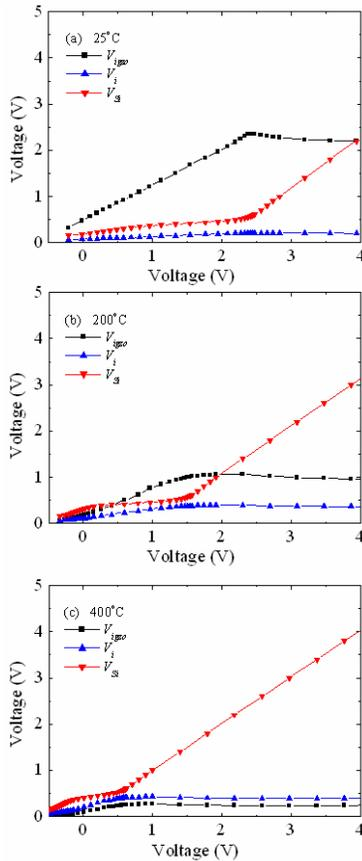


Fig. 8. Detailed partial voltages of IGZO/Si heterojunction diodes fabricated at various temperature: (a) 25 °C; (b) 200 °C; (c) 400 °C.

5. Summary and conclusions

IGZO films grown on equally doped p-type silicon substrates of (100) orientation at 25 °C, 200 °C and 400 °C provide rectifying heterocontacts and maximum quantum

efficiency as high as 87.97%. S-shape photocurrents are observed for all the PDs, which could not be fitted into conventional photoelectric model neglecting IL. As shown in the I-V characteristic of IGZO/Si PDs in the darkness, the nonideal ideality factor at forward bias indicates that negatively charged interface states exist. As reason, a photocurrent model with IL considered is developed here, in which, the photocurrent flowing through PD is induced by conduction electrons captured by interface states which have sufficient energy to flow through the IGZO barrier and both the recombination currents at IL and SCR are also considered. It is found that our photocurrent model with IL fits the I-V characters of PDs fabricated at different temperatures very well. It is indicated that the photocurrent limitation is ultimately caused by the low electron mobility and deficient of conduction electrons at IGZO/Si IL. Electron accumulation occurs at IL leads to low partial voltage of silicon and both these two reasons lead to high recombination at IL and SCR which directly limits the photocurrent under low reverse bias and causes the S-shape photocurrent. With increasing the deposition temperature, the impurity concentration of IGZO increases and leads to less partial voltage falling on IGZO barrier, consequently, the photocurrent saturates under lower reverse bias voltage.

Acknowledgments

This work was supported by the National Natural Science Foundation of China (61040061) and the “973” National Key Basic Research Program of China (Grant No. 2007CB310500) and the Project supported by Hunan Provincial Natural Science Foundation of China (11JJ2034)

References

- [1] S. Mridha, D. Basak, JAP. **101**, 083102 (2007).
- [2] H. Y. Kim, J. H. Kim, Y. J. Kim, Optical Materials. **17**, 141 (2001).
- [3] Hongxia Qi, Qingshan Li, Caifeng Wang, Vacuum. **81**, 943 (2007).
- [4] Min-Suk Oh, Sang-Ho Kim, Tae-Yeon Seong, APL. **87**, 122103 (2005).
- [5] J. Y. Lee, Y. S. Choi, J. H. Kim, Thin Solid Films. **420**, 112 (2002).
- [6] J. P. Donnelly, A. G. Milnes, PROC. IEEE. **113**, 1468 (1966).
- [7] T. L. Tansley, S. J. T. Owen, IEEE Transaction on Electron Devices. ED-23, 1123 (1976).
- [8] T. L. Tansley, S. J. T. Owen, JAP. **55**, 454 (1984).
- [9] Thomas L. Paoli, Peter A. Barnes, APL. **28**, 714 (1976).
- [10] Wolfgang W. Gärtner, Physical Review. **116**, 84 (1959).
- [11] J. Reichman, JAP. **36**, 574 (1980).
- [12] J. Tersoff, Physical Review B. **30**, 4874 (1984).

*Corresponding author: yunzeng@hnu.edu.cn